Uncertainties Estimation of Measurement Devices by Using Finite Element Method

Marija M. Cundeva-Blajer[1] and Ljupco S. Arsov[2]

***Abstract* – In this paper an advanced CAD methodology for metrological uncertainties estimation of two electromagnetical measurement devices will be presented. The metrological characteristics of a 20 kV combined current-voltage instrument transformer, as well as of an electrical steel sheet testing device-Epstein frame will be determined by using an original program package developed at the Faculty of Electrical Engineering and Information Technologies-Skopje, based on the finite element method, FEM-3D. The FEM-3D outputs will be input data for further metrological improvement, of the test devices.**

***Keywords* – Finite element method, Epstein frame, instrument transformer.**

I. INTRODUCTION

This paper will provide a study of several inaccuracy sources that appear in the electromagnetic measurement devices. Two metrological objects of analysis: 20 kV combined current-voltage instrument transformer (CCVIT) and electrical steel sheet testing apparatus-Epstein frame (EF) will be studied. The measurement devices must comply with the rigorous metrological standards such as IEC 60404-2, [1] and IEC 60044-2, [2]. The metrological uncertainty of the electromagnetic testing devices must be estimated as exactly as possible. These devices are complex electromagnetic systems, which are highly non-linear and their analysis by using the analytical methods introduces a lot of approximations and their design will be with very high metrological uncertainty. So the application of the numerical methods, like the finite element method, for the analysis of the electromagnetic fields phenomena is indispensable.

II. ELECTROMAGNETIC FIELD ANALYSIS

A. FEM-3D

The magnetic field distribution in closed and bounded systems (such as the EF and the CCVIT) is described by the system of Maxwell's equations. After the magnetic vector potential $\vec{A}$ as an auxiliary quantity is introduced, the magnetic field distribution is expressed by the Poison's non-linear partial differential equation:

$$\frac{\partial}{\partial x}\left(\vec{\nu}(\vec{B})\frac{\partial \vec{A}}{\partial x}\right)+\frac{\partial}{\partial y}\left(\vec{\nu}(\vec{B})\frac{\partial \vec{A}}{\partial y}\right)+\frac{\partial}{\partial z}\left(\vec{\nu}(\vec{B})\frac{\partial \vec{A}}{\partial z}\right)=-\vec{j}(x,y,z) \quad (1)$$

where $\vec{B}$ is the magnetic flux density, $\vec{\nu}$ the magnetic reluctivity and $\vec{j}(x,y,z)$ the volume current density. The analyzed devices are heterogeneous and non-linear with prescribed boundary conditions and eq. 1 can be solved by numerical methods, only. The magnetic field analysis is done by an original and universal program package FEM-3D developed at the Faculty of Electrical Engineering and Information Technologies-Skopje (FEIT), [3].

The FEM-3D program comprises five main modules: G1-automatic mesh generator; G2-flux plot; G3-input definition of boundary conditions, material magnetic properties, magnetizing current sources; G4-magnetic field distribution calculator; G5-electromagnetic characteristics calculator. The 3D iterative finite element method calculations are done by taking into account the magnetic anisotropy and the different magnetic reluctivities along the co-ordinate axes, due to the lamination of the magnetic cores of the devices.

B. Case Study No. 1-Epstein Frame

The Epstein frame forms an unloaded transformer comprising a primary magnetising winding, a secondary voltage winding and electrical steel sheet as test specimen, as given Fig. 1.

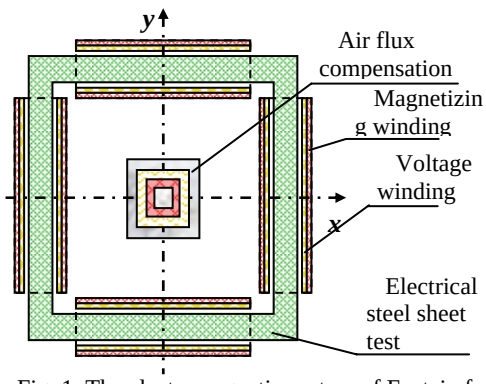

Fig. 1. The electromagnetic system of Epstein frame

Systematic errors which exist at the Epstein frame must be eliminated or reduced. However, the Epstein frame is a highly non-linear electromagnetic system, therefore for its proper design and analysis the numerical methods such as the finite element method, are indispensable, [3].

The initial analysis of the Epstein frame electromagnetic

[1]Marija M. Cundeva-Blajer is with the Faculty of Electrical Engineering and Information Technologies, Karpos II bb, POBox 574, 1000 Skopje, Macedonia, E-mail: mcundeva@etf.ukim.edu.mk

[2]Ljupco S. Arsov is with the Faculty of Electrical Engineering and Information Technologies, Karpos II bb, POBox 574, 1000 Skopje, Macedonia, E-mail: ljarsov@etf.ukim.edu.mk

system is done by application of the classical analytical transformer theory. However, that is an approximate calculation because of the numerous neglections that are included. Some of these approximations which introduce systematic errors are:

- constant magnetic path length l_m=0,94 m, like in [1];
- approximate magnetic field distribution;
- not exactly calculated leakage fluxes in the air.

For appropriate geometrical and mathematical modeling of the EF, its compound configuration is divided into 7 layers along the axial axis of the frame, as follows: the magnetizing winding (1. and 7. layer), the voltage winding (2. and 6. layer), the isolation+air (3. and 5. layer), the magnetic core of the specimen examined by the frame (4. layer). Computations are carried out for various magnetic polarization and for different grades of reference specimen of electrical steel sheet. The reference specimen parameters are given in Table I.

TABLE I
MAIN PARAMETERS OF THE THREE REFERENCE SPECIMEN GRADES

	Grade A	Grade B	Grade C
Grade according to IEC 60404-8-7, 1998	M95-23P 5	M110-27P 5	M140-30S 5
Mass *m* [kg]	0,5551	0,5973	0,7100
Number of strips *n*	40	36	40
Cross-section surface per branch $A_{j,br}$ [cm^2]	0,6479	0,6971	0,8287
Stacking factor k_{fe}	0,945	0,950	0,955
Active mass m_a [kg]	0,4659	0,5013	0,5959
Thickness *d* [mm]	0,216	0,258	0,276
Height *h* [mm]	4,320	4,644	5,520

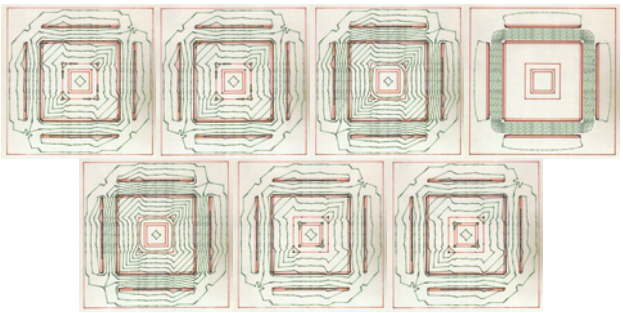

Fig. 2. Magnetic flux plots in the 7 cross-sectional layers along the z-axis of the EF with electrical steel sheet (magnetic core) at J_m = 0,8 T

After the non-linear iterative FEM-3D calculations of the magnetic vector potential are accomplished, the flux plots of the magnetic field distribution in the seven cross-sections along the z-axis of the Epstein frame three-dimensional domain are derived, as displayed in Fig. 2.

C. Case Study No. 2-Combined Instrument Transformer

The combined current-voltage instrument transformer (CCVIT) comprises four windings and two magnetic cores in one housing. The initial CCVIT (voltage measurement core VMC ratio $20000\,V/\sqrt{3} : 100\,V/\sqrt{3}$ and current measurement core CMC ratio 100 A : 5 A) analysis is done by application of the analytical transformer theory. Still, this is a very complex electromagnetic system in highly non-linear regime and with two cores mutually magnetically coupled, as shown in Fig. 3.

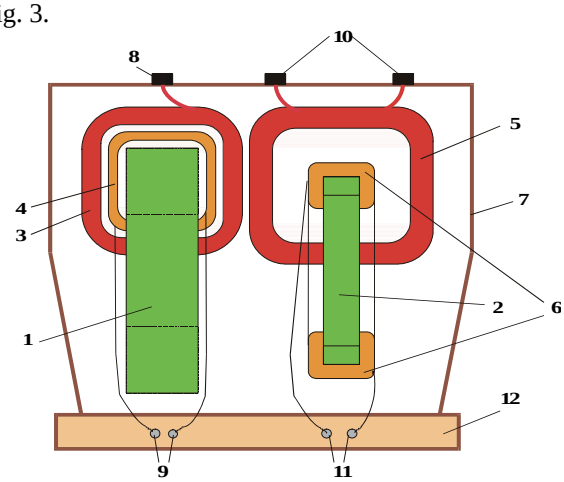

Fig. 3. Electromagnetic system of the 20 kV CCVIT

(1-VMC magnetic core; 2-CMC magnetic core; 3-VMC high voltage primary winding; 4-VMC low voltage secondary winding; 5-CMC high current primary winding; 6-CMC low current secondary winding; 7-common isolation housing; 8-high voltage socket lit; 9-low voltage socket lits; 10-primary current socket lits; 11-secondary current socket lits; 12-isolation base)

The CCVIT electromagnetic phenomena is analysed by FEM-3D, [3]. The objective of the FEM-3D analysis is the estimation of the four CCVIT metrological parameters:

- p_u VMC voltage error
- p_i CMC current error
- δ_u VMC phase displacement error
- δ_i CMC phase displacement error.

They are calculated through the following procedure:

No load voltage error:

$$p_{0u} = -100 \cdot (r_{1eu} \cdot g_{0eu} + x_{\sigma 1eu} \cdot b_{0eu}) \quad (2)$$

No load phase displacement error:

$$\delta_{0u} = 3440 \cdot (r_{1eu} \cdot b_{0eu} - x_{\sigma 1eu} \cdot g_{0eu}) \quad (3)$$

Voltage error introduced by the load:

$$p_{tu} = -100 \cdot ((r_{1eu} + r_{2eu}) \cdot g_{eu} + (x_{\sigma 1eu} + x_{\sigma 2eu}) \cdot b_{eu}) \quad (4)$$

Phase displacement error introduced by the load:

$$\delta_{tu} = 3440 \cdot ((r_{1eu} + r_{2eu}) \cdot b_{eu} - (x_{\sigma 1eu} + x_{\sigma 2eu}) \cdot g_{eu}) \quad (5)$$

VMC total voltage error:

$$p_u = p_{0u} + p_{tu} \quad (6)$$

VMC total phase displacement error:

$$\delta_u = \delta_{0u} + \delta_{tu} \quad (7)$$

$\vec{Z}_{2i}$ is total CMC secondary circuit impedance:

$$Z_i'' = \sqrt{(R_{ti} + R_{2i})^2 + (X_{ti} + X_{\sigma 2i})^2} = \sqrt{R_i''^2 + X_i''^2} \quad (8)$$

$$tg\boldsymbol{\beta}_{2i} = \frac{X_{ti} + X_{\boldsymbol{\sigma}2i}}{R_{ti} + R_{2i}} = \frac{X''_i}{R''_i} \qquad (9)$$

CMC current error:

$$p_i \approx -\frac{I''_{0i}}{I''_{1i}} \cdot cos(\boldsymbol{\varphi}_{fei} - \boldsymbol{\beta}_{2i}) \cdot 100\% \qquad (10)$$

CMC phase displacement error:

$$\boldsymbol{\delta}_i \approx 3440 \cdot \frac{I''_{0i}}{I''_{1i}} \cdot sin(\boldsymbol{\varphi}_{fei} - \boldsymbol{\beta}_{2i})[\text{min}] \qquad (11)$$

where: $cos\boldsymbol{\varphi}_{fei} = \frac{P_{fei}}{S_{fei}}$ and

- r_{1eu} and $x_{\sigma 1eu}$ are the resistance and the leakage reactance of the VMC primary winding (per turn);
- r_{2eu} and $x_{\sigma 2eu}$ are the resistance and the leakage reactance of the VMC secondary winding (per turn);
- R_{1i} and $X_{\sigma 1i}$ are the resistance and the leakage reactance of the CMC primary winding (total);
- R_{2i} and $X_{\sigma 2i}$ are the resistance and the leakage reactance of the CMC secondary winding (total).

TABLE II
FEM-3D CALCULATED VMC PRIMARY WINDING LEAKAGE REACTANCES PER TURN

U_u/U_{ru}	Only VMC	0	0,2	0,4	0,6	0,8	1,0	1,2
I_i/I_{ri}	$x_{\sigma 1eu}$ [μΩ]							
0,2	91,61	91,22	83,48	69,41	58,30	47,10	36,16	25,3
0,4	92,12	92,09	86,56	81,01	75,46	69,84	64,38	59,0
0,6	91,28	91,29	87,61	83,88	80,19	76,48	72,78	69,2
0,8	91,51	91,49	88,73	85,97	83,17	80,40	77,62	74,9
1,0	91,61	91,64	89,40	88,20	84,97	82,74	80,54	78,4
1,2	91,81	91,79	89,95	88,11	86,26	84,40	82,54	80,8

TABLE III
FEM-3D CALCULATED VMC SECONDARY WINDING LEAKAGE REACTANCES PER TURN

U_u/U_{ru}	Only VMC	0	0,2	0,4	0,6	0,8	1,0	1,2
I_i/I_{ri}	$x_{\sigma 2eu}$ [μΩ]							
0,2	63,58	63,31	57,94	48,17	40,46	32,69	25,10	17,56
0,4	63,93	63,91	60,07	56,22	52,37	48,47	44,68	40,95
0,6	63,35	63,35	60,80	58,21	55,66	53,08	50,51	48,04
0,8	63,51	63,49	61,58	59,66	57,72	55,80	53,87	52,02
1,0	63,58	63,60	62,04	61,21	58,97	57,42	55,89	54,40
1,2	63,72	63,71	62,43	61,15	59,87	58,58	57,28	56,06

TABLE IV
FEM-3D CALCULATED CMC PRIMARY WINDING LEAKAGE REACTANCES PER TURN

I_i/I_{ri}	Only CMC	0	0,2	0,4	0,6	0,8	1,0	1,2
U_u/U_{ru}	$x_{\sigma 1ei}$ [μΩ]							
0,2	28,09	27,75	27,47	27,21	26,91	26,68	26,39	26,18
0,4	28,10	27,76	27,62	27,50	27,35	27,21	27,09	26,96
0,6	28,09	27,75	27,67	27,58	27,48	27,39	27,30	27,22
0,8	28,11	27,76	27,70	27,63	27,56	27,49	27,43	27,37
1,0	28,10	27,75	27,69	27,64	27,58	27,52	27,48	27,42
1,2	27,99	27,66	27,59	27,58	27,51	27,45	27,43	27,38

TABLE V
FEM-3D CALCULATED CMC SECONDARY WINDING LEAKAGE REACTANCES PER TURN

I_i/I_{ri}	Only CMC	0	0,2	0,4	0,6	0,8	1,0	1,2
U_u/U_{ru}	$x_{\sigma 2ei}$ [μΩ]							
0,2	8,910	8,801	8,713	8,630	8,537	8,462	8,370	8,305
0,4	8,913	8,806	8,760	8,723	8,676	8,630	8,592	8,551
0,6	8,911	8,803	8,775	8,747	8,716	8,688	8,661	8,633
0,8	8,915	8,806	8,785	8,764	8,741	8,720	8,699	8,681
1,0	8,914	8,801	8,784	8,767	8,749	8,730	8,715	8,698
1,2	8,877	8,772	8,752	8,747	8,726	8,705	8,701	8,685

The leakage reactances of the four windings can be calculated by numerical methods only, because they include the non-linearity of the magnetic cores and their mutual electromagnetic coupling. By using the program package FEM-3D they have been iteratively derived and are given in Tables II-V.

III. POSTPROCESSING OF THE FINITE ELEMENT METHOD ANALYSIS RESULTS

A. Case Study No. 1-Epstein Frame

After FEM-3D calculations of the magnetic vector potential are accomplished, by using numerical integration, and the exact 3D magnetic field distribution in the frame is derived. In the IEC standard 60404-2, [1] the effective magnetic path length l_m is taken as constant and equal to 0,94 m. Still, in [4] it has been shown that it depends on the material as well as on the magnetic polarisation. The l_m has been derived for three reference specimen of electrical steel sheet as shown in Fig. 4.

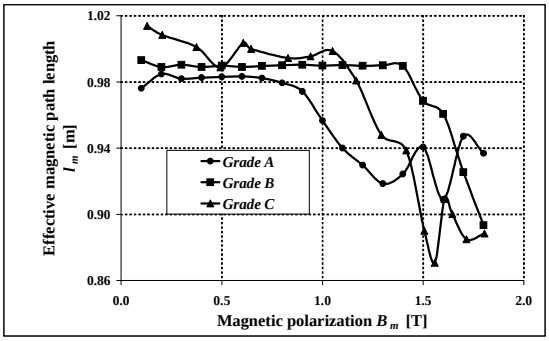

Fig. 4. FEM-3D calculated effective magnetic path length l_m via the magnetic polarization

The precise finite element estimation of the magnetic path length l_m of the EF enables reduction of the measurement uncertainties during the process of experimental testing of the electrical steel sheet properties (e. g. the specific power losses P_s=f(J_m) or the magnetic characteristics H=f(J_m)).

B. Case Study No. 2-Combined Instrument Transformer

The FEM-3D derived values of the CCVIT leakage reactances are introduced in the CCVIT metrological parameters given in Tables VI-XI.

TABLE VI

VMC NO LOAD VOLTAGE ERROR

I_i/I_{ri}	only VMC	0	0,2	0,4	0,6	0,8	1,0	1,2
U_u/U_{ru}	p_{u0} [%]							
0,2	-0,34	-0,34	-0,31	-0,26	-0,22	-0,18	-0,15	-0,11
0,4	-0,28	-0,28	-0,26	-0,25	-0,23	-0,22	-0,20	-0,19
0,6	-0,24	-0,24	-0,23	-0,23	-0,22	-0,21	-0,20	-0,19
0,8	-0,22	-0,22	-0,22	-0,21	-0,21	-0,20	-0,19	-0,19
1,0	-0,21	-0,21	-0,20	-0,20	-0,20	-0,19	-0,19	-0,18
1,2	-0,21	-0,21	-0,20	-0,20	-0,19	-0,19	-0,19	-0,18

TABLE VII

VMC VOLTAGE ERROR INTRODUCED BY THE LOAD

I_i/I_{ri}	only VMC	0	0,2	0,4	0,6	0,8	1,0	1,2
U_u/U_{ru}	p_{ul} [%]							
0,2	-12,35	-12,3	-11,5	-9,91	-8,69	-7,46	-6,26	-5,07
0,4	-6,20	-6,20	-5,90	-5,59	-5,29	-4,98	-4,68	-4,38
0,6	-4,10	-4,10	-3,97	-3,83	-3,70	-3,56	-3,43	-3,30
0,8	-3,08	-3,08	-3,01	-2,93	-2,85	-2,78	-2,70	-2,63
1,0	-2,47	-2,47	-2,42	-2,39	-2,32	-2,27	-2,23	-2,18
1,2	-2,06	-2,06	-2,03	-1,99	-1,96	-1,93	-1,89	-1,86

TABLE VIII

VMC VOLTAGE ERROR

I_i/I_{ri}	only VMC	0	0,2	0,4	0,6	0,8	1,0	1,2
U_u/U_{ru}	p_u [%]							
0,2	-12,69	-12,6	-11,8	-10,2	-8,92	-7,65	-6,41	-5,18
0,4	-6,48	-6,48	-6,16	-5,84	-5,52	-5,20	-4,88	-4,57
0,6	-4,35	-4,35	-4,21	-4,06	-3,92	-3,77	-3,63	-3,49
0,8	-3,31	-3,31	-3,23	-3,15	-3,07	-2,98	-2,90	-2,82
1,0	-2,68	-2,68	-2,63	-2,60	-2,52	-2,47	-2,42	-2,37
1,2	-2,27	-2,27	-2,23	-2,20	-2,16	-2,12	-2,08	-2,05

TABLE IX

VMC NO LOAD PHASE DISPLACEMENT ERROR

I_i/I_{ri}	only VMC	0	0,2	0,4	0,6	0,8	1,0	1,2
U_u/U_{ru}	δ_{u0} [min]							
0,2	-4,99	-4,96	-4,41	-3,39	-2,59	-1,79	-1,00	-0,22
0,4	-4,77	-4,77	-4,41	-4,04	-3,67	-3,33	-2,94	-2,59
0,6	-4,95	-4,95	-4,70	-4,45	-4,21	-3,90	-3,71	-3,48
0,8	-4,72	-4,72	-4,54	-4,37	-4,19	-4,02	-3,84	-3,68
1,0	-4,48	-4,48	-4,34	-4,27	-4,08	-3,95	-3,82	-3,69
1,2	-4,43	-4,43	-4,32	-4,21	-4,11	-3,99	-3,88	-3,78

TABLE X

VMC PHASE DISPLACEMENT ERROR INTRODUCED BY THE LOAD

I_i/I_{ri}	only VMC	0	0,2	0,4	0,6	0,8	1,0	1,2
U_u/U_{ru}	δ_{ul} [min]							
0,2	-407	-405	-366	-295	-240	-183	-128	-73,9
0,4	-205	-205	-191	-177	-163	-149	-135	-121
0,6	-135	-135	-129	-122	-116	-110	-104	-98,3
0,8	-101	-101	-98,3	-94,8	-91,3	-87,8	-84,3	-80,9
1,0	-81,5	-81,5	-79,3	-78,1	-74,8	-72,6	-70,4	-68,2
1,2	-68,1	-68,1	-66,5	-65,0	-63,4	-61,9	-60,3	-58,8

TABLE XI

VMC PHASE DISPLACEMENT ERROR

I_i/I_{ri}	only VMC	0	0,2	0,4	0,6	0,8	1,0	1,2
U_u/U_{ru}	δ_u [min]							
0,2	-412	-410	-371	-299	-242	-185	-129	-74,1
0,4	-209	-209	-195	-181	-166	-152	-138	-124
0,6	-140	-140	-133	-127	-120	-114	-108	-101
0,8	-106	-106	-102	-99,2	-95,5	-91,8	-88,1	-84,6
1,0	-86,0	-86,0	-83,6	-82,4	-78,9	-76,5	-74,2	-71,9
1,2	-72,5	-72,5	-70,8	-69,2	-67,5	-65,9	-64,2	-62,6

TABLE XI

CMC CURRENT ERROR

U_u/U_{ru}	only CMC	0	0,2	0,4	0,6	0,8	1,0	1,2
I_i/I_{ri}	p_i [%]							
0,2	-1,16	-1,16	-1,16	-1,16	-1,16	-1,16	-1,16	-1,16
0,4	-0,89	-0,89	-0,89	-0,89	-0,89	-0,89	-0,89	-0,89
0,6	-0,75	-0,75	-0,75	-0,75	-0,75	-0,75	-0,75	-0,75
0,8	-0,68	-0,68	-0,68	-0,68	-0,68	-0,68	-0,68	-0,68
1,0	-0,68	-0,68	-0,68	-0,68	-0,68	-0,68	-0,68	-0,68
1,2	-0,64	-0,64	-0,64	-0,64	-0,64	-0,64	-0,64	-0,64

TABLE XI

CMC PHASE DISPLACEMENT ERROR

U_u/U_{ru}	only CMC	0	0,2	0,4	0,6	0,8	1,0	1,2
I_i/I_{ri}	δ_i [min]							
0,2	8,47	8,54	8,59	8,64	8,69	8,74	8,79	8,83
0,4	3,82	3,87	3,89	3,90	3,92	3,95	3,96	3,98
0,6	2,59	2,63	2,64	2,65	2,66	2,67	2,68	2,69
0,8	0,84	0,87	0,88	0,89	0,90	0,90	0,91	0,92
1,0	0,50	0,54	0,54	0,55	0,55	0,56	0,57	0,57
1,2	0,17	0,20	0,21	0,21	0,22	0,23	0,23	0,23

IV. CONCLUSION

In this paper an original methodology for measurement devices uncertainty estimation, by using the finite element method, has been given. The derived results can be further used for metrologically improved design of the Epstein frame and the combined instrument transformer.

REFERENCES

[1] IEC (International Electrotechnical Commission) 60404-2, 1996: Magnetic Materials, Part 2: Methods of measurement of magnetic properties of electrical steel sheet and strip by means of an Epstein frame, Geneve, 1996.

[2] IEC (International Electrotechnical Commission) 60044-2, 1980: Instrument transformers, Part 3: Combined transformers, Geneve, 1980.

[3] M. Cundev, L. Petkovska, The Weighted Residuals Method for Electromagnetic Field Problems in Electrical Machines, Proc. of the 32nd Universities Power Engineering Conference UPEC'97, Vol. 2, UMIST, Manchester, UK, pp.934-937, 1997.

[4] M. Cundeva, L. Arsov, Experimental Verification of the Results from the FEM-3D Magnetic Field Analysis of Epstein Frame, Studies in Applied Electromagnetics and Mechanics, vol. 22, IOS Press Ohmsha, Amsterdam, pp.379-384, 2002.